RISK MANAGEMENT APPLIED TO AEROSPACE ENGINEERING DESIGN

Irina-Carmen ANDREI[*], Gabriela-Liliana STROE[*,], Sorin BERBENTE[*,**], Vasile PRISACARIU[***], Emil COSTEA[*], Ionel POPESCU[****], Octavian Ioan FILIPESCU[*****]**

[*]INCAS – National Institute for Aerospace Research "Elie Carafoli", Bucharest, Romania (andrei.irina@incas.ro, stroe.gabriela@incas.ro, berbente.sorin@incas.ro, costea.emil@incas.ro)
[**]"Politehnica" University of Bucharest, Faculty of Aerospace Engineering, Romania
[***]"Henri Coandă" Air Force Academy, Brașov, Romania (prisacariu.vasile@afahc.ro)
[****]STRAERO – Institute for Theoretical and Experimental Analysis of Aeronautical Structures, Bucharest, Romania (ionel.popescu@straero.ro)
[*****]"Politehnica" University of Bucharest, Faculty of Mechanical Engineering and Mechatronics, Romania, (ranma50387@yahoo.com)

DOI: 10.19062/2247-3173.2023.24.16

***Abstract**: The intent of this paper is to present applications of risk management to aerospace engineering design; the study was focused on composite materials design and manufacturing of parts, assemblies from aircraft and spacecraft, such as aerostructures, fuselage, aircraft wings and controls, jet engines parts such as fan blades, widely used in aerospace engineering. The use of composites in aerospace engineering provides significant reduction of costs for manufacturing, technology and operation, provided adequate management. Management in composites design, manufacturing and technology may allow to achieving performance and cost-effectiveness for such aerospace engineering parts, which are critical from the safety standpoint.*

***Keywords**: Risk Management, Aerospace Engineering, Composite Materials, Design, Manufacturing, Safety.*

1. INTRODUCTION

Design of aircraft and space product constructions must be compliant with the safety standards specifically stated in regulations for the commercial and military aircraft industry, prior to all other criteria.

Then, subordinated to safety standards are the general and specific design criteria, like: geometry, loads, mechanical stress, thermal stress, reliability, then manufacturing, operating and maintenance costs, and the last but not the least, aesthetics. Improved properties as high strength and stiffness, combined with low density can be provided by the use of composite materials when compared with bulk materials, allowing for a weight reduction in the finished product/ assembly/ part.

Composite materials are widely used today in aerospace engineering, due to their provided advantages, such as: lighter weight, the ability to tailor the layup for optimum strength and stiffness, improved fatigue life, corrosion resistance, long working life, lower density with respect to steel alloys, high strength to weight ratio, low coefficient of

thermal expansion, five times stronger than steel, reduced assembly costs due to fewer detail parts and fasteners in case of mastering good design practice.

On the other hand, disadvantages of composites must be taken into account and contingency plans must be provided, where applicable or available; disadvantages of composites refer to: high raw material costs and usually high fabrication and assembly costs, adverse effects of both temperature and moisture, poor strength in the out of plane direction where the matrix carries the primary load, susceptibility to impact damage and delimitations or ply separations, greater difficulty in repairing composite parts when compared to metallic structures.

Aircraft design represents an intricate exhaustive task, since it involves specific design of aircraft structure, propulsion system, aircraft controls, engine controls, avionics, Auxiliary Power Unit (APU), landing gear and other parts.

The design cycle of an aircraft can cover a duration of more than 20 years, because it is an iterative process, which supposes a step by step development following a Technology Readiness Assessment (TRA) that examines program concepts, technology requirements, and demonstrated technology capabilities.

Technology Readiness Levels (TRLs) are based on a scale from 1 to 9, with 9 being the most mature technology, as detailed in Table 1, [18].

Table 1 – Technology Readiness Levels (TRLs), [18]

TRL	**NASA usage, [19]**	**European Union, [20]**
1	Basic principles observed and reported	Basic principles observed
2	Technology concept and/or application formulated	Technology concept formulated
3	Analytical and experimental critical function and/or characteristic proof-of concept	Experimental proof of concept
4	Component and/or breadboard validation in laboratory environment	Technology validated in lab
5	Component and/or breadboard validation in relevant environment	Technology validated in relevant environment (industrially relevant environment in the case of key enabling technologies)
6	System/subsystem model or prototype demonstration in a relevant environment (ground or space)	Technology demonstrated in relevant environment (industrially relevant environment in the case of key enabling technologies)
7	System prototype demonstration in a space environment	System prototype demonstration in operational environment
8	Actual system completed and "flight qualified" through test and demonstration (ground or space)	System complete and qualified
9	Actual system "flight proven" through successful mission operations	Actual system proven in operational environment (competitive manufacturing in the case of key enabling technologies; or in space)

Mathematical Modeling and Numerical Simulations have an important role in design and concept development. Design improvements and/or design optimizations often result as consequences of feedback from Mathematical Modeling and Numerical Simulations.

This paper presents some of the most significant and common topics encountered in aerospace engineering design and the approach to problem's study and solving from the standpoint of associated risk management. The proposed topics for this paper are: 1/ thermo-gas-dynamics of turbojet engines, 2/ design and reverse engineering in case of axial compressor and fan rotor blades, 3/ guidelines of risk management customized for aerospace engineering design.

For each of these topics, an approach of Risk Management in the meaning of Risk Intelligence will be addressed. The steps assume the successive completion of the following stages: 1/ Risk Identification, 2/ Risk Assessment, from the standpoint of impact and likelihood, 3/ Prioritization of risks, 4/ pointing out the actions to be taken, which can be one of the following options: a/ tolerate, b/ treat, c/ substitute, d/ terminate.

Risk Intelligent is a holistic approach of Risk Management, considered globally, that is looking at the entire system as a whole, not just focusing on some parts of the system, without also considering the determining relationships and interactions between the various parts of the general system. Risk Intelligent can be considered as a tool for Active Control serving Risk Management to control and maintain the adjusted balance between risks and reward. The ultimate goal of Risk Intelligent is to create added value by assuming risks and enabling simultaneously to protect, keep and maintain the values already accumulated.

2. TOPIC #1: THERMO-GAS-DYNAMICS OF TURBOJET ENGINES

Problem Statement and Framework: The thermo-gas-dynamics analysis of the turbojet engine is carried out in order to achieve the following objectives:

1/ to calculate the performances of the turbojet engine at Design Regime and to do its performance prediction at Off-Design Regime;

2/ to investigate the engine operating regimes, concluded within the determined turbojet engine's Operation Maps (Altitude Map, Velocity Map, Rotor Speed Map) and engine's Universal Map, based on turbojet engine performances, previously calculated;

3/ to carry on the Steady State Analysis, which consists in the investigation of the engine’s operating regimes and equilibrium states, based on the performances of the turbojet engine calculated in previous steps;

4/ to provide calculated data as input to carry on the Transient State Analysis, which reveals the dynamic behavior of the turbojet engine and further enables to complete the study of turbojet engine automate control. The results from Transient State Analysis enable the design of jet engine’s automate control and further, the design and management of the aircraft engine controls.

The design of the turbojet engine supposes the completion of the thermo-gas-dynamics analysis performed initially at the level of the entire engine, as a system and then at the level of turbojet engine main parts (air inlet & intake, compressor system, combustion chamber, turbine and exhaust unit), Fig. 1.

The accuracy of the results is strongly influenced by the Mathematical Modeling of the turbojet engine and the assumptions related with the turbojet engine’s operation. The accuracy is influenced by the level of the approximation, that is the way the assumptions are taken into consideration.

The numerical accuracy depends on the numerical methods and algorithms chosen for solving numerically the equations that define the turbojet engine's mathematical model. Only few equations can be solved analytically.

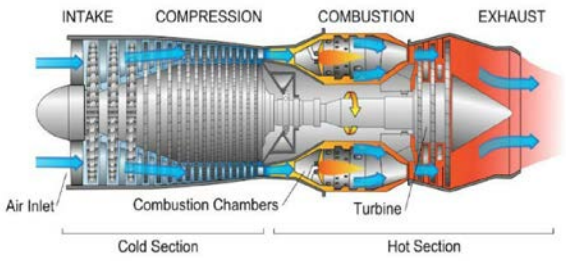

FIG. 1 Turbojet Engine (TJE), [22]

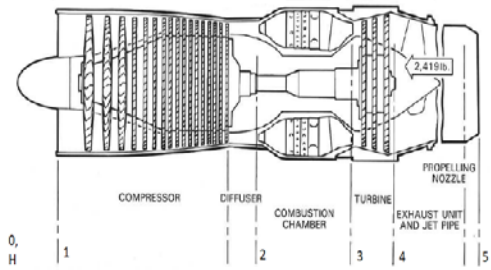

FIG. 2 Definition of Turbojet Engine Stations, [21]

The study is concluded by the results obtained from Numerical Simulations.

This paper is focused on the turbojet performance analysis, with the application to the TJ100 single spool turbojet engine, as Test Case, [23-26].

Turbojet engine Performance Prediction refers to the calculation of the turbojet engine's performances: Thrust [N], Specific Thrust [N*s/kg] and Specific Fuel Consumption [kg/N/h] – TSFC, for the entire range of parameters: flight altitude [m] and flight velocity V [m/s] or flight Mach number, as expressed by the Aircraft's Flight Envelope and for all the operating regimes of the turbojet engine.

The algorithm for determining the Brayton Diagram provides eventually the turbojet engine's performances: Thrust [N], Specific Thrust [N*s/kg] and Specific Fuel Consumption [kg/N/h].

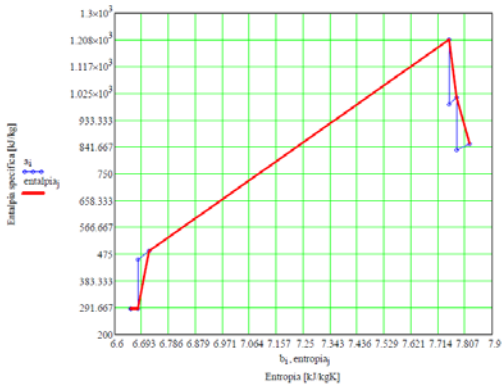

a/ **Design Regime**:
Altitude H = 0, Flight Mach number = 0,
Flight Velocity V = 0 [m/s]

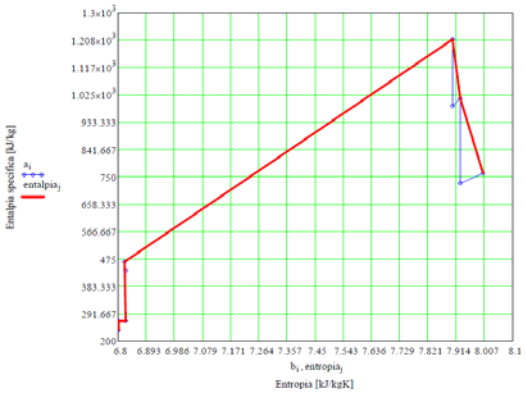

b/ **Off-Design Regime**:
Altitude H = 8 [km], Flight Mach number = 0.8,
Flight Velocity V = 246 [m/s]

FIG. 3 Brayton Diagram, calculated for the **Design Regime** (*left*) and an **Off-Design Regime** (*right*), in case of TJ 100 Turbojet Engine, [23-26]

The Brayton Diagram express the turbojet engine's thermodynamic cycle and it is usually described by the coordinates: specific entropy [kJ/kg/K] and specific enthalpy [kJ/kg]. The turbojet engine stations, defined as shown in Fig. 2, match the points within the field of the Brayton Diagram.

In blue contours is the thermodynamic evolution of the ideal flow along core engine flow path, with the supposed assumptions: the fluid is an ideal gas, one species, adiabatic processes, no losses.

In red contours is the thermodynamic evolution of the core engine real flow, modeled with the supposed assumptions: the fluid is a perfect gas, two species, adiabatic processes, considered losses due to drag, friction, local turbulence, the thermodynamic system representing the engine model is considered open.

The Brayton Diagram presented in Fig. 3-a was calculated for the Design Regime, at SLS, ISA conditions (i.e. "*fixed point*", which usually means altitude H = 0 [km] and flight velocity V = 0 [m/s] or flight Mach number =0), Fig. 3-a, while the Brayton Diagram exposed in Fig. 3-b was determined for a selected Off-Design Regime, (Altitude H = 9 [km], Mach number = 0.8, which gives Flight Velocity V = 246 [m/s]).

Main input data for calculating the Brayton Diagram and the performances of the TJ 100 turbojet engine: Thrust [N], Specific Thrust [N*s/kg] and Specific Fuel Consumption [kg/N/h]:

Pressure ratio =5.0, Airflow Mass Rate = 1.74 [kg/s], Turbine Inlet Temperature T3T = 1123 [K].

$\pi_c^* = \frac{p_2^*}{p_1^*}$ $\dot{M}_a = 1.74\ \left[\frac{kg}{s}\right]$ $T_3^* = 1123\ [K]$

Other turbojet engine parameters:

$\eta_c^* = 0.85$ - Adiabatic efficiency on compression
$\eta_t^* = 0.89$ - Adiabatic efficiency on turbine expansion
$\eta_m = 1$ - Mechanical (shaft) efficiency, =1 / single spool construction
$\sigma_{da}^* = 0.92$ - Pressure loss at engine intake
$\sigma_{ca}^* = 0.98$ - Pressure loss in combustor
$\xi_{ca} = 0.998$ - Combustion efficiency
$\varphi_{ar} = 0.940$ - Exhaust nozzle velocity loss

The **Mathematical Model** of the turbojet engine describing its behavior as close to reality is based on the following set of **Assumptions**:

- the working fluid is considered perfect gas,
- two species:
  // **air** // - from engine intake to compressor, stations: 0-1-2;
  // **burned gas** // - within combustor, turbine and exhaust unit, stations: 2-3-4-5;
- fuel specific power, for JET A, JET A1 and/or JET B (aviation kerosene): $P_{CI} = 43500\ \left[\frac{kJ}{kg}\right]$,
- ratio of specific heat $k = \frac{C_p}{C_v}$, see Table 1.
- constant pressure specific heat $C_p\ [\frac{kJ}{kgK}]$:
- gas constant $R\ \left[\frac{kJ}{kgK}\right]$; the relation between *R* and C_p is: $C_p = R\ \cdot \frac{k}{k-1}$

Table 1 Properties of the working fluids

Fluid	*k*	C_p [kJ/kg/K]	*R* [J/kg/K]
Air	1.4	1.005	287.3
Burned Gas	1.33	1.165	288.4

The **Mathematical Model** for computing the turbojet engine performances is defined by the following equations:

- SLS, ISA conditions: $p_0 = 1.01325\ [bar]$ (1), $T_0 = 288\ [K]$ (2) and $i_0 = C_p \cdot T_0\ [kJ/kg]$, (3)
- conditions at engine inlet (intake) - station 0 (SLS) or H (flight):
- *if* H = 0 [km] *then* $p_1^* = \sigma_{da}^* \cdot p_0\ [bar]$, (4), $T_1^* = T_0\ [K]$ (5), and $i_1^* = C_p \cdot T_1^*\ [kJ/kg]$ (6),
  if H > 0 *then* $p_1^* = p_H^* \cdot p_0\ [bar]$ (7), $T_1^* = T_H^*\ [K]$ (8) and $i_1^* = C_p \cdot T_1^*\ [kJ/kg]$ (9),

where $T_H = T_0 - 6.5 \cdot H\ [km],\ [K]$ (10) and $p_H = p_0 \cdot \left(\frac{T_H}{T_0}\right)^{5.2553}$ (11)

$$and\ T_H^* = T_H + \frac{V^2}{2 \cdot C_p} \quad (12)$$

$$\text{or } T_H^* = T_H \cdot \left(1 + \frac{(k-1)}{2} \cdot Mach^2\right) \quad (13)$$

$$and\ p_H^* = p_H \cdot \left(1 + \frac{(k-1)}{2} \cdot Mach^2\right)^{\left(\frac{k-1}{k}\right)} \quad (14)$$

- dynamic pressure ratio:

$$\pi_d^* = \frac{p_H^*}{p_H} = \left(\frac{T_H^*}{T_H}\right)^{\left(\frac{k-1}{k}\right)} = \left(1 + \frac{(k-1)}{2} \cdot Mach^2\right)^{\left(\frac{k-1}{k}\right)} = \left(\Theta(Mach)\right)^{\left(\frac{k-1}{k}\right)} \quad (15)$$

- dynamic pressure ratio at Off-Design Regime (Mach number = 0.9) is:

$$\pi_d^* = \left(1 + \frac{(k-1)}{2} \cdot Mach^2\right)^{\left(\frac{k-1}{k}\right)} = \left(1 + \frac{(1.4-1)}{2} \cdot 0.8^2\right)^{\left(\frac{1.4-1}{1.4}\right)} = 1.035$$

- conditions at compressor inlet-station 1^*: $p_1^* = \sigma_{da}^* \cdot p_H^*$ (16) , $T_1^* = T_H^*$ (17) , $i_1^* = i_H^*$ (18)
- conditions at combustor inlet - station 2^*:

$$p_2^* = \pi_c^* \cdot p_1^* \quad (19), \qquad i_2^* = i_1^* \cdot \left(1 + \frac{\left((\pi_c^*)^{\frac{k-1}{k}} - 1\right)}{\eta_c^*}\right) \quad (20), \quad T_2^* = \frac{i_2^*}{C_p} \quad (21)$$

- conditions at turbine inlet - station 3^*:

$p_3^* = \sigma_{ca}^* \cdot p_2^*$ (22),· T_3^* being given, then: $i_3^* = C_{pg} \cdot T_3^*$ (23)

- fuel flow coefficient (from energy balance eqn. in combustor):

$$m_c = \frac{(i_3^* - i_2^*)}{(\xi_{ca} \cdot P_{ci} - i_3^*)} \quad (24)$$

- burned gas flow coefficient (from mass balance eqn. in combustor):

$$m_g = 1 + m_c \quad (25)$$

- *fuel flow coefficient:* $m_c = \frac{\dot{M}_c}{\dot{M}_a}$ *(26)*
- burned gas flow coefficient: $m_g = \frac{\dot{M}_g}{\dot{M}_a}$ (27)
- conditions at turbine exit - station 4^*:

$i_4^* = i_3^* - l_t^*$ (28), $T_4^* = \frac{i_4^*}{C_{pg}}$ (29); $p_4^* = \frac{\delta_t^*}{p_3^*}$ (30),

- where δ_t^* is the pressure ratio in turbine, and it comes out from the expression of specific work in turbine. $\delta_t^* = \left(1 - \frac{l_{t\_id}^*}{i_3^*}\right)^{-\left(\frac{kg}{kg-1}\right)}$ (31)
- conditions at nozzle exit - station 5:

case: full exhaust nozzle expansion: $p_5 = p_H$ (32) , then the thrust obtained is maximum

case: partial exhaust nozzle expansion:

$p_5 = p_{cr} < p_H$ (34), $p_{cr} = \left(\frac{2}{kg+1}\right)^{\left(\frac{kg}{kg-1}\right)} \cdot p_4^*$ (35)

- velocity of expelled gas c_5 [m/s], (36):

$$c_5 = \varphi_{ar} \cdot \sqrt{2 \cdot \left\{ \begin{array}{c} \left[i_3^* \cdot \left(1 - \pi_d^* \cdot \sigma_{da}^* \cdot \pi_c^* \cdot \sigma_{ca}^*\right)^{-\left(\frac{kg-1}{kg}\right)} \right] - \\ -i_1^* \cdot \left[\frac{(\pi_c^*)^{\frac{k-1}{k}} - 1}{\eta_c^* \cdot \eta_t^* \cdot \eta_m} \right] \end{array} \right\}} \quad (36)$$

- the turbojet engine performances:
  - specific thrust: $F_{sp} = m_g \cdot c_5 - V, \left[\frac{Ns}{kg}\right]$, (37)
  - thrust: $F = F_{sp} \cdot \dot{M}_a\ , [N]$, (38)
  - specific fuel consumption: $C_{sp} = \frac{3600 \cdot m_c}{F_{sp}}, \left[\frac{kg}{Nh}\right]$ (39)

- the influence of altitude, flight Mach number and rotor speed on Airflow Mass Rate and compressor pressure ratio:
  - Airflow Mass Rate (40) is influenced by the change of altitude and flight Mach number, by the means of the variation of compressor pressure ratio, dynamic pressure ratio and the ratio of static pressures at altitude H [km] versus SLS, ISA conditions:

$$\dot{M}_a = \dot{M}_{a\,0} \cdot \frac{\pi_c^*}{\pi_{c\,0}^*} \cdot \pi_d^* \cdot \frac{p_H}{p_0} \tag{40}$$

  - specific work on compression (41) changes with the square of rotor speed (42)

$$l_c^* = l_{c\,0}^* \cdot \bar{n}^2 \tag{41}$$

  - rotor speed % (42) represents the ratio of speeds at operating versus nominal engine regime:

$$\bar{n} = \frac{n}{n_{NOMinal}} \tag{42}$$

  - the relations between specific work of compressor, compressor pressure ratio, intake enthalpy and rotor speed, are (43) for SLS, ISA conditions and (44) for the flight at altitude:

$$l_{c\,0}^* = i_0 \cdot \left(\frac{\left(\pi_{c\,0}^*\right)^{\frac{k-1}{k}} - 1}{\eta_{c\,0}^*} \right) \tag{43}$$

$$l_c^* = i_H^* \cdot \left(1 + \frac{\left((\pi_c^*)^{\frac{k-1}{k}} - 1\right)}{\eta_c^*} \right) \tag{44}$$

  - the influence of altitude, flight Mach number and rotor speed on compressor pressure ratio (45) - (48) is deduced from relations (43), (44) and (41); the ratio of compressor efficiencies at operating regime versus nominal can be taken about 1.0 (as initial approximation or in case that the universal compressor map is not available):

$$\pi_c^* = \left[1 + \left(\left(\pi_{c\,0}^*\right)^{\frac{k-1}{k}} - 1 \right) \cdot \frac{i_0}{i_H^*} \cdot \bar{n}^2 \cdot \frac{\eta_c^*}{\eta_{c\,0}^*} \right]^{\left(\frac{k}{k-1}\right)} \tag{45}$$

$$\pi_c^* = \left[1 + \left(\left(\pi_{c\,0}^*\right)^{\frac{k-1}{k}} - 1 \right) \cdot \frac{i_0}{i_H^*} \cdot \bar{n}^2 \right]^{\left(\frac{k}{k-1}\right)} \tag{46}$$

$$\pi_c^* = \left[1 + \left(\left(\pi_{c\,0}^*\right)^{\frac{k-1}{k}} - 1 \right) \cdot \frac{i_0}{i_H^*} \cdot \bar{n}^2 \right]^{\left(\frac{k}{k-1}\right)} \tag{47}$$

$$\pi_c^* = \left[1 + \frac{l_{c\_id}}{i_H^*} \cdot \bar{n}^2 \right]^{\left(\frac{k}{k-1}\right)} \tag{48}$$

The results of Numerical Simulations for the Design Regime and Off-Design Regime, in case of the TJ 100 turbojet engine are summarized in Table 2:

Table 2 – Results of Performance Prediction at Design Regime and Off-Design Regime

Pressure Ratio				5
Airflow Mass Rate [kg/s]				1.74 [kg/s]
Fuel Flow Mass Rate [kg/s]				0.0185 [kg/s]
Turbine Inlet Stagnation Temperature T3T [K]				1123 [K]
Turbine Exit Stagnation Temperature T4T [K]				956 [K]
Velocity of expelled gas c_5 [m/s]				524 [m/s]
Performance Prediction at Design Regime (H=0, Mach =0)				
Thrust [N] ; Thrust [daN]		1000.881 [N]		100.09 [daN]
Specific Thrust [N*s/kg]		574.21 [N*s/kg]		574.21 [N*s/kg]
Specific Fuel Consumption [kg/N/h]		0.1077 [kg/N/h]		1.077 [kg/daN/h]
Flight Regime: H [km], Mach number				
H [km]		9 [km]		9 [km]
Mach		0.8		0.8
V [m/s]		246 [m/s]		246 [m/s]
The influence of the flight regime on turbojet engine parameters (Pressure Ratio, Airflow Mass Rate, Fuel Flow Mass Rate) and performances				
Pressure Ratio	5.0	5.517	5.7123	5.7123
Airflow Mass Rate [kg/s]	1.74	1.2501	0.9366	0.9366 [kg/s]
Fuel Flow Mass Rate [kg/s]	0.0185	0.0338	0.0259	0.0259 [kg/s]
Velocity of expelled gas c_5 [m/s]				708 [m/s]
Performance Prediction at Off- Design Regime (H=9, Mach = 0.8)				
Thrust [N] ; Thrust [daN]		494.85 [N]		≅ 49.50 [daN]
Specific Thrust [N*s/kg]		474.06 [N*s/kg]		474.06 [N*s/kg]
Specific Fuel Consumption [kg/N/h]		0.1343 [kg/N/h]		1.343 [kg/daN/h]

Altitude Map is presented in Fig. 4 and Velocity Map is depicted in Fig. 5.

Rotor Speed Map, illustrated in Fig. 6, was calculated for the following rotor speed regimes:

- rotor speed: $\bar{n} = 1.05$ → Emergency Max. Regime → 105% *n*
- rotor speed: $\bar{n} = 1.00$ → Design Regime → 100% *n*
- rotor speed: $\bar{n} = 0.91$ → Cruise Regime → 91% *n*
- rotor speed: $\bar{n} = 0.84$ → Lowered Cruise Regime → 84% *n*
- rotor speed: $\bar{n} = 0.50$ → Ground Idle Regime → 50% *n*

where: $\bar{n} = \frac{n_{Operating\ \ Regime}}{n_{Design\ \ Regime}}$ is the non-dimensional rotor speed.

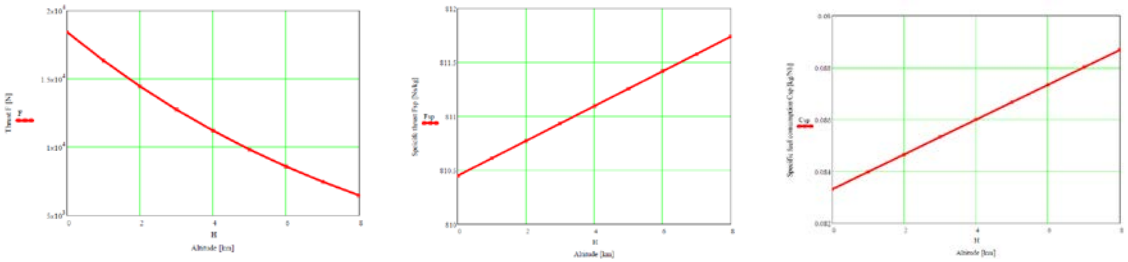

Thrust | Specific Thrust | Specific Fuel Consumption

FIG. 4 Altitude Map

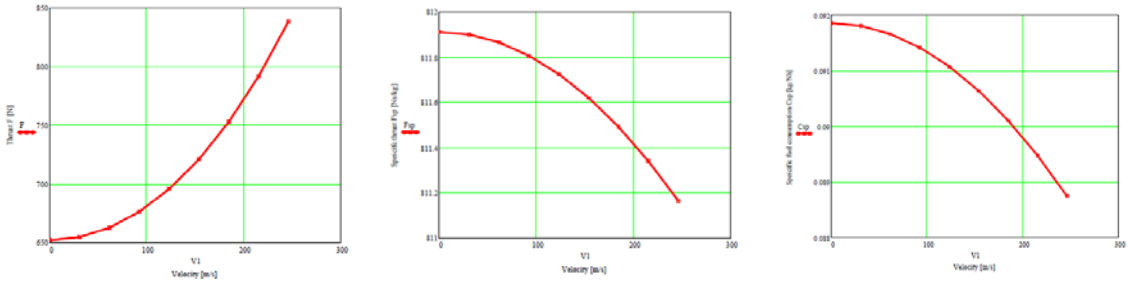

Thrust | Specific Thrust | Specific Fuel Consumption

FIG. 5 Velocity Map

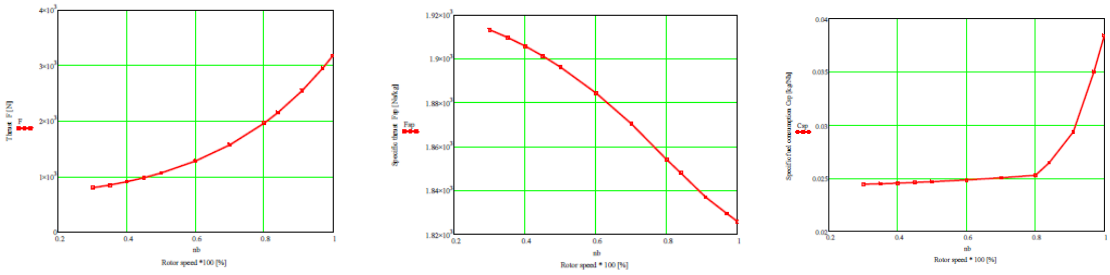

Thrust | Specific Thrust | Specific Fuel Consumption

FIG. 6 Rotor Speed Map

3. TOPIC #2: DESIGN AND REVERSE ENGINEERING IN CASE OF AXIAL COMPRESSOR AND FAN ROTOR BLADES

The design of the blade airfoil results from the kinematics of the blade cascade; the velocity vectors determine the deflection of the fluid flow and by way of consequence the twist of the blade airfoil.

Reverse Engineering enables to obtain the geometry of a 3D body.

In case of the axial compressor rotor blade, presented in Fig, 7, direct measurements provided the following values for the Blade chord = 30 [mm] and Blade-max_thickness = 3 [mm].

Since the blade chord is constant along the blade span, then the airfoil surface is generated by the translation of the NACA 4-digits Airfoil from blade hub to blade tip.

By using Airfoil Tools, [27] following the selection of the NACA 2412, result the non-dimensional coordinates (X, Y) and the real (dimensional) coordinates (Xr, Yr) of the NACA 2412 Airfoil:

Xr [mm] = X * Blade chord
Yr [mm] = Y * Blade max_thickness

View from Pressure Surface | View from Sucction Surface | View from Blade Tip

FIG. 7 Axial Compressor Rotor Blade

The significance of the digits in case of the NACA 2412 Airfoil is:

- Max Camber = 2 (%); first digit can range between 0 to 9.5%
- Max Camber position = 40 (%); second digit can range between 0 to 90%
- Thickness = 12 (%), third & fourth digit can range between 1 to 40%

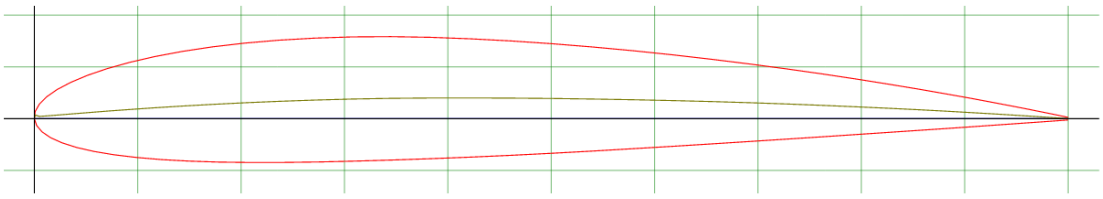

FIG. 8 NACA 2412 Airfoil (M=2.0% P=40.0% T=12.0%), [27]

NACA 2412 Airfoil using the NACA 4-digit Airfoil generator, [27], results as illustrated in Fig. 8, with Max thickness 12% at 30.7% chord and Max camber 2% at 38.3% chord.

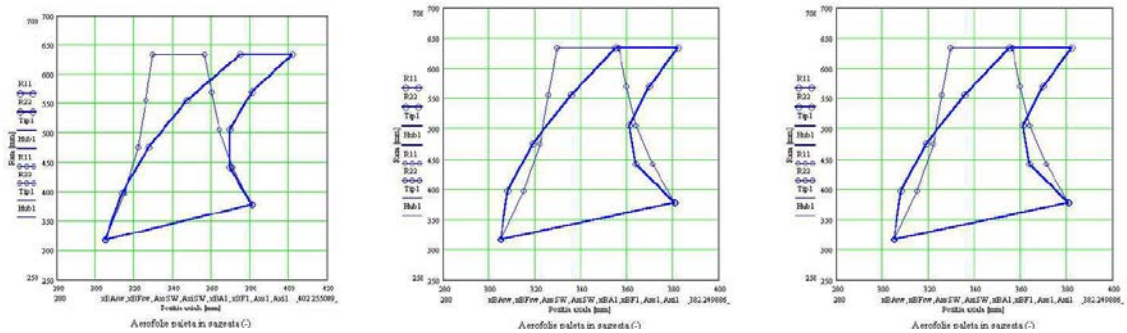

$\chi[°] = [-30\,;\,-15\,;\,-4\,;1\,;0\,]$ $\chi[°] = [-18\,;\,-7\,;\,2\,;5\,;0\,]$ $\chi[°] = [\,0\,;\,5\,;\,8\,;6\,;0\,]$

FIG. 9 Numerical Simulations of Sweep Effect Applied to Axial Compressor Rotor, [28]

In other situations, the blade chord is not constant along the blade span, but the airfoil surface can still be generated by the translation of a NACA Airfoil from blade hub to blade tip.

An effective method to increase the accuracy consists in considering different NACA airfoils for more intermediate blade spanwise sections, as well as for the blade hub and blade tip.

In case of higher velocity airflow blade cascades, NACA 65 Series Airfoils behave better and therefore are more appropriated.

In case of rotor fan blades, for large bypass turbofan engines for commercial aircraft, while running the engine at higher rotor speed regimes (cruise and design regimes), then shock waves may occur at blade tip, followed by boundary layer detachment and later re-attachment. This is a risk situation and can be avoided or mitigated from blade design, following the application of sweep effect to different stations located blade spanwise.

Numerical Simulations of sweep effect applied to an axial compressor rotor blade was performed and thorough details have been presented in [28]. In Fig. 9 are concluded the Numerical Simulations for different blade spanwise distributions of sweep angle $\chi[°]$; in light blue contours is represented the reference blade, while in dark blue contours is depicted the blade with sweep effect.

4. TOPIC #3: GUIDELINES OF RISK MANAGEMENT CUSTOMIZED FOR AEROSPACE ENGINEERING DESIGN

Technology advancements in case of large turbofan engines for commercial aircrafts:

1/ increased engine thrust due to enlargement of fan blade tip diameter resulting an increase of ingested airflow,

2/ application of sweep to fan blades such that to avoid the occurrence of shock waves at blade tip while the engine is operated at high rotational speeds, Fig. 10, Fig. 11,

3/ expanding the use of composites to fan parts (rotating blades, guiding vanes, casings), Fig. 12, allowed advanced aerodynamic design of fan blades and important decline of weight, and in the same time, as composites provide higher strength and stiffness, allowed product life cycle extension and the diminishing of costs related to manufacturing and maintenance.

FIG. 10 Fan blade design evolution, [29]

FIG. 11 GE 90 fan blade, [30]

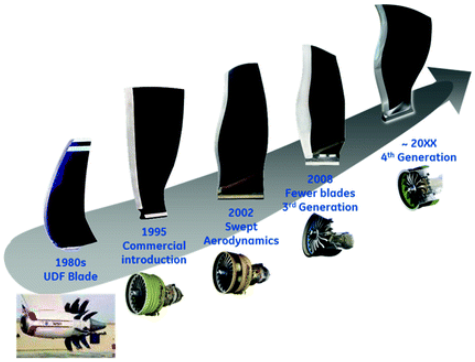

FIG. 12 Evolution of fan blade design, [31]

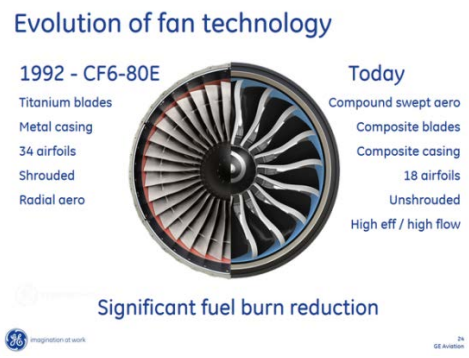

FIG. 13 Evolution of fan technology, [32]

The advantages provided by a composite fan blade, Fig. 11, to large bypass turbofan engines for commercial aircraft, are expressed by the following facts:

1. Titanium leading edge, which ensure ingestion protection, serviceability, replaceable,
2. Polyurethane coating, that brings reduced wear,
3. Composite airfoil, due to higher strength and stiffness, increases the capability to support higher stresses and loads with lowered weight,
4. Low crush stress, does not require lubrification.

FIG. 14 Design and technology advances in jet engines, GE NX Turbofan Engine, [33]

The use of composites in jet engines, Fig. 13, Fig. 14, Fig. 15, can be successfully applied for the engine cold parts, like air inlet, fan, and partially to LPC – Low Pressure compressor, fuel system, FADEC system, fuel tanks.

FIG. 15 Advanced LEAP turbofan engines, [34]

Key elements of design and technology advances in jet engines are highlighted in Fig. 14 for the GE NX large bypass turbofan engine and in Fig. 15 for the CFM International's advanced LEAP product line, which is the engine of choice to power the Airbus A320neo, the Boeing 737 MAX, and the COMAC C919.

Advanced technology of new LEAP turbofan engines enables to set new standards in utilization, reliability, and performance. Since CFM's first LEAP engines entered revenue service in August 2016, the fleet has demonstrated world-class daily utilization rates and delivered a 15 percent improvement in fuel efficiency, along with significant reductions in noise and emissions signatures - all while maintaining CFM's industry-leading reliability and overall cost of ownership, [34].

The design and technology advances in jet engines emerged from continuous search for performance improvement and as well as the need to mitigate or to completely avoid risks in aircraft and jet engine operation.

Management of assumed risks in case of damage tolerance is used in aircraft design. Damaged tolerance concept represents an assumed risk from the standpoint of the safety management of loads and stresses to which the aircraft is subjected. Examples for design load cases and resulting stresses in case of commercial aircraft are shown in Fig. 16. In Fig. 17 are shown levels of damage tolerance assessments.

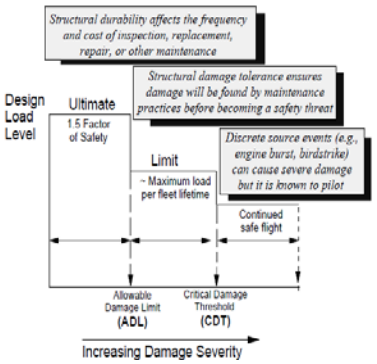

FIG. 16 Design load and damage considerations for durability and damage tolerance, [16].

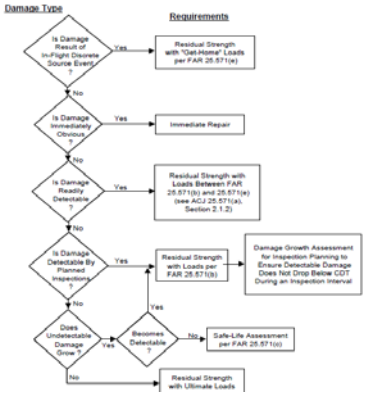

FIG. 17 Levels of damage tolerance assessments, [16]

In case of composites, and especially carbon fiber composites, the "No Crack Growth" Concept of Carbon Fiber Reinforced Polymer CFRP is one of the most important Damage Tolerance Requirements. For the aircraft safety operation, health monitoring HM on composite material structures CMS is crucial.

The lessons learned from the primary and secondary composite structures, up to B 787, provided solid information and validations for the implementation of a variety of composite materials structural design constructions and fabrication methods. Summarizing the lessons learned on composite use in aerospace engineering, there were successfully used:

- application of innovative design and technology advances in jet engines;
- advanced technology of new LEAP turbofan engines that enables to set new standards in utilization, reliability, and performance;
- application of advanced composites to aircraft and fiberglass rotor technology;
- carbon fiber epoxy laminates, for all fuselage sections, main wing box, horizontal and vertical stabilizer boxes;
- carbon fiber laminate materials, for wing leading edge slats and trailing edge flaps;
- carbon sandwich constructions, for secondary structures (rudder, elevators, winglets, nacelle cowlings)
- glass fiber epoxy, other composites or similar materials, for several fairings on the wing stabilizers, radome, wing-to-fuselage fairings,
- metal alloys, for the leading edge of the nacelles, for the reason of serving as a good heat conductor, for thermal anti-icing,
- titanium based alloys, for some joints and internal substructures like heavy-load carrying fittings, and for most of the landing gear components,
- advanced composites as fiberglass rotor technology, helicopters and rotor blade helicopters.

Table 3 – Examples of composite use in aircraft and helicopter parts

Aircraft Parts	Composite Materials, Composite Technology	Helicopter Parts	Composite Materials, Composite Technology
Leading edges	RTM (Resin Transfer Molding)	Main rotor hub plate	Prepreg curing
Clips	TP Stamping	Tail rotor blade	RTM (Resin Transfer Molding)
Structural interior parts	RTM, Curing	Blade	Prepreg Curing

Thermoplastic rotating parts	Consolidation	Structural parts	RTM, Curing
Stiffeners	HDF (Hot Drape Forming)		
Preforms	HDF		
TP consolidated plates	Consolidation		
Honeycomb structural parts	Compression & Curing		
Turbine blade	Hot forming, Consolidation, RTM		

Before a new aircraft can obtain FAA certification, numerous tests must be performed in order to validate composite materials performance and to verify structural integrity. The test set includes Static Test, fatigue Test, Ground and Flight Tests.

Analysis and testing ensure safety and reliability must be performed increasing the levels of complexity, from material specimens, elements, assemblies, components up to airplane.

5. CONCLUSIONS

This paper is structured on three main parts: 1/ analysis of turbojet engine performance prediction at Design Regime and Off-Design Regimes, based on the thermo-gas-dynamics of turbojet engine; 2/ design and reverse engineering in case of axial compressor and fan rotor blades, design and technology advances in jet engines, 3/ guidelines of risk management customized for aerospace engineering design.

The topics considered for this study are the most significant and common encountered in aerospace engineering design. Each study subject was developed such that to highlight the appropriate solution and to perform Risk Management, following the successive completion of the stages:

1/ Risk Identification,

2/ Risk Assessment, from the standpoint of impact and likelihood,

3/ Prioritization of risks, 4/ pointing out the actions to be taken, which can be one of the following options: a/ tolerate, b/ treat, c/ substitute, d/ terminate. The options for Risk mitigation are: a/ tolerate, b/ treat, while the options to avoid or to eliminate risks are: c/ substitute, d/ terminate.

6/ Risk monitor and report, to develop the Risk Register, which is a database of information on risks;

7/ Risks reviewed periodically.

Risk Intelligent is a holistic approach of Risk Management, considered globally, that is looking at the entire system as a whole, not just focusing on some parts of the system, without also considering the determining relationships and interactions between the various parts of the general system. Risk Intelligent can be considered as a tool for Active Control serving Risk Management to control and maintain the adjusted balance between risks and reward. The ultimate goal of Risk Intelligent is to create added value by assuming risks and enabling simultaneously to protect, keep and maintain the values already accumulated.

ACKNOWLEDGEMENT:

This research is supported by INCAS - National Institute for Aerospace Research Elie Carafoli, as a beneficiary of the Project - Technological Development Platform for Green Technologies in Aviation and Ecological Manufacturing with Superior Added Value, TGA

- TECHNOLOGIES FOR GREEN AVIATION, financed by the Competitiveness Operational Program 2014-2020 (POC), POC/448/1/1/Large R&D Infrastructures, SMIS CODE 127115, Contract of Financing no. 313 / 14.07.2020 funded by Romanian Ministry of Research, Innovation and Digitization.

REFERENCES

[1] Newman Dava J., *Interactive Aerospace Engineering and Design*, Massachusetts Institute of Technology, John D. Anderson Jr., University of Maryland, Consulting Editor, McGraw-Hill Series in Aeronautical and Aerospace Engineering, McGraw-Hill Higher Education, ISBN 0–07–234820–8, ISBN 0–07–112254–0 (ISE), 2002;

[2] D, M. Bushnell, *Industrial Design in Aerospace/Role of Aesthetics*, National Aeronautics and Space Administration, Langley Research Center, Hampton, Virginia 23681-2199, August 2006;

[3] ***, *Advanced Design Problems in Aerospace Engineering*, Volume 1: Advanced Aerospace Systems, Edited by Angelo Miele, Rice University Houston, Texas and Aldo Frediani, University of Pisa, Pisa, Italy, KLUWER ACADEMIC PUBLISHERS, NEW YORK, BOSTON, DORDRECHT, LONDON, MOSCOW, 2004, KLUWER ACADEMIC PUBLISHERS, NEW YORK, 2003, eBook ISBN: 0-306-48637-7, Print ISBN: 0-306-48463-3;

[4] F. Bouissiere, C. Cuiller, P.-E. Dereux, C. Malchair, C. Favi, G. Formentini, (2019), *Conceptual Design for Assembly in Aerospace Industry: A Method to Assess Manufacturing and Assembly Aspects of Product Architectures*, in Proceedings of the 22nd International Conference on Engineering Design (ICED19), Delft, The Netherlands, 5-8 August 2019, pp. 2961-2970, DOI:10.1017/dsi.2019.303, Published online by Cambridge University Press;

[5] A.J Keane, J.P Scanlan, *Design Search and Optimization in Aerospace Engineering*, Article in Philosophical Transactions of The Royal Society A Mathematical Physical and Engineering Sciences, November 2007, DOI: 10.1098/rsta.2007.2019, Source: PubMed, The Royal Society Publishing, Series: Mathematical, Physical and Engineering Sciences, Published: 22 May 2007 https://doi.org/10.1098/rsta.2007.2019 ;

[6] ***, *Design and Manufacturing Guideline for Aerospace Composites*, NASA Series: Preferred Reliability Practices, NASA Guideline No. GD-ED-2205;

[7] D. Edberg, W. Costa, *Design of Rockets and Space Launch Vehicles*, ISBN (print): 978-1-62410-593-7, Publication Date: August 21, 2020, https://doi.org/10.2514/4.105937;

[8] E.R. Johnson, *Aerospace Structures*, Blacksburg, VA: Kevin T. Crofton Department of Aerospace and Ocean Engineering, https://doi.org/10.21061/AerospaceStructures, 2022, Licensed with CC BY NC-SA 4.0. https://creativecommons.org/licenses/by-nc-sa/4.0 ;

[9] Curtis E. Larsen, Ivatury S. Raju, *Moving Aerospace Structural Design Practice to a Load and Resistance Factor Approach*, NASA Langley Research Center, Hampton, Virginia, https://ntrs.nasa.gov/api/citations/20160007733/downloads/20160007733.pdf ;

[10] NASA/SP-2007-6105 Rev1, *Systems Engineering Handbook*, National Aeronautics and Space Administration, NASA Headquarters, Washington, D.C. 20546, December 2007;

[11] O.T. Pleter, *Introduction to Aerospace Engineering*, Air Navigation Series, Bucureşti: Editura Universităţii Româno-Britanice, 2009, ISBN: 978-606-8163-00-0, Printed in ROMANIA by Monitorul Oficial R. A. Printing House; 2nd Digital Edition published by: Brainbond, Bucureşti, România, 2013, www.brainbond.ro, 1st Edition published by: Editura Universităţii Româno-Britanice, Bucureşti, 2009, Spl. Independenţei 319B, 060044 Bucureşti (România), tel. (+40 21) 221 5840, (+4) 0723 300510, fax. (+40 21) 221 5815 office@theU.ro www.theU.ro ;

[12] S. Quinn, *Engineering Drawing Practices*, Volume I of II, Aerospace and Ground Support Equipment, KSC-GP-435, Volume I, Revision H, Engineering Directorate, John F. Kennedy Space Center, NASA, August 11, 2020;

[13] Editors: S. Kishore Kumar (Gas Turbine Research Establishment, Bengaluru, India), Indira Narayanaswamy (M. S. Ramaiah, University of Applied Sciences, Bengaluru, India), V. Ramesh (National Aerospace Laboratories, Bengaluru, India), *Design and Development of Aerospace Vehicles and Propulsion Systems*, Proceedings of SAROD 2018, Conference Proceedings published in 2021;

[14] R. C. Alderliesten, *Introduction to Aerospace Structures and Materials*, Delft University of Technology, Delft, The Netherlands, ISBN E-pub: 978-94-6366-077-8, ISBN hardcopy: 978-94-6366-074-7, ISBN PDF: 978-94-6366-075-4;

[15] Andreas Aronsson, *Design, Modeling and Drafting of Composite Structures*, Master of Science Programme Thesis, Luleå University of Technology, Department of Applied Physics and Mechanical

Engineering, Division of Computer Aided Design, Sweden, 2005:060 CIV, ISSN: 1402-1617, ISRN: LTU-EX—05/60—SE;
[16] MIL-HDBK-17-3F, Department of Defense Handbook, Composite Materials Handbook, Volume 3 of 5, Polymer Matrix Composites. Materials Usage, Design and Analysis, USA, 17 June 2002;
[17] General Electric GE 90 Turbofan Engine;
[18] https://en.wikipedia.org/wiki/Technology_readiness_level, 19/05/2023;
[19] "Technology Readiness Level Definitions" (PDF). *nasa.gov*. Retrieved 6 September 2019. This article incorporates text from this source, which is in the public domain;
[20] "Technology readiness levels (TRL); Extract from Part 19 - Commission Decision C(2014)4995" (PDF). *ec.europa.eu. 2014*. Retrieved 11 November 2019. Material was copied from this source, which is available under a Creative Commons Attribution 4.0 International License;
[21] Rolls Royce, *The Jet Engine*, Rolls Royce plc, 1986, 5th edition, Derby, England, ISBN 0902121 235;
[22] https://images.news18.com/ibnlive/uploads/2020/01/Turbojet.png , 19/05/2023;
[23] I.C. Andrei, A. Toader, G. Stroe, F. Frunzulica, *'Performance analysis and dinamic modeling of a Single-Spool Turbojet Engine'*, 11 th International Conference in Nonlinear Problems in Aviation and Aerospace, ICNPAA 2016 WORLD CONGRESS, THOMSON REUTERS - ISI, ISBN: 978-0-7354-1464-8, ISSN: 0094-243X, DOI: 10.1063/1.4972597, WOS: 000399203000005;
[24] C. Nae, I.C. Andrei**,** G. Stroe, S. Berbente, *'Mathematical Modeling and Numerical Simulations for Performance Prediction in Case of the Turbojet Engine'*, 17th International Conference of Numerical Analysis and Applied Mathematics, ICNAAM 2019, AIP Conference Proceedings 2293, WOS;
[25] I.C. Andrei, M.L. Niculescu, M.V. Pricop, A. Cernat, *Study of the Turbojet Engines as Propulsion Systems for the Unmanned Aerial Vehicles*, Scientific Research and Education in the Air Force International Conference AFASES 2016, Volume I (2016), pp.115-126, "Henri Coanda" Air Force Academy, https://www.afahc.ro/afases/ volum_afases_2016_II.pdf , DOI:10.19062/2247-3173.2016.18.1.15 , Scientific papers 2016 Volume I, ISSN, ISSN-L: 2247-3173, Indexed: EBSCO, COPERNICUS;
[26] I.C. Andrei, C. Rotaru, M.C. Fadgyas, G. Stroe, M.L. Niculescu, *Numerical Investigation of Turbojet Engine Thrust Correlated with the Combustion Chamber's Parameters*, Scientific Research and Education in the Air Force International Conference AFASES 2017, Volume I (2017), pp.23-34, "Henri Coanda" Air Force Academy, http://www.afahc.ro/afases/volum_afases_2017_I.pdf, DOI:10.19062/2247-3173.2017.19.1.2 , Scientific papers 2017 Volume I, ISSN, ISSN-L: 2247-3173, Indexed: EBSCO, COPERNICUS;
[27] Airfoil Tools, http://airfoiltools.com/airfoil/naca4digit, http://airfoiltools.com/search/index, 09/05/2022;
[28] A.I. Carmen, Teza de Doctorat: *„Cercetari cu privire la studiul curgerii prin retelele de palete de compresor axial si posibilitati de imbunatatire a performantelor, cu aplicatii la motoarele aeroreactoare"/ „Researches regarding the study of flow in axial compressor blade cascades and potential means for performance improvement, with applications to jet engines"*, Universitatea POLITEHNICA din Bucuresti, facultatea de Inginerie Aerspatiala, 2007, 237 pagini, Coordinator Stiintific: Prof. Dr. Ing. Corneliu Berbente, 533.6(043.2); 621.51.001; 5(043.2); 621.45(043.2); B-UP 1, http://www.library.pub.ro/doc/teze/tezedoctorat2008.pdf;
[29] https://duckduckgo.com/?t=ffab&q=fan+blade+design+evolution&iax=images&ia=images&iai=https%3A%2F%2Fleehamnews.com%2Fwp-content%2Fuploads%2F2016%2F11%2FCFM-blades.png, 19/05/2023;
[30] https://duckduckgo.com/?t=ffab&q=ge90+fan+blade&iax=images&ia=images&iai=https% 3A% 2F%2Fs-media-cache-ak0.pinimg.com%2Foriginals%2F23%2F38%2F6a% 2F23386a619cf05e8d2bfd6717a7412a54.jpg, 19/05/2023;
[31] https://media.springernature.com/lw785/springer-static/image/chp:10.1007%2F978-3-319-23419-9_3/MediaObjects/314564_1_En_3_Fig10_HTML.gif, 19/05/2023;
[32]https://duckduckgo.com/?q=ge+90+fan+blade+design+&t=ffab&iar=images&iax=images&ia=images&iai=https%3A%2F%2Fqph.fs.quoracdn.net%2Fmain-qimg-4cc1790a9392b901e6b846f2853f4ba6, 19/05/2023;
[33] http://brianjohnsonaviation.weebly.com/uploads/1/4/1/4/1414163/1945687_orig.jpg, 19/05/2023;
[34]https://duckduckgo.com/?q=ge+90+fan+blade+design+&t=ffab&iar=images&iax=images&ia=images&iai=http%3A%2F%2Fleehamnews.com%2Fwp-content%2Fuploads%2F2012%2F02%2Fleap_3.jpg%3Fw%3D300, 19/05/2023.